Dual dynamic voltammetry with rotating ring–disk electrodes

S. Vesztergom, M. Ujvári and G.G. Láng*

Eötvös Loránd University of Budapest – Laboratory of Electrochemistry & Electroanalytical Chemistry
H-1117 Budapest, Pázmány Péter sétány 1/A, Hungary

Abstract

A novel voltammetric technique based on the simultaneous dynamic potential control of both the disk and the ring electrodes of an RRDE is presented. The method of dual cyclic voltammetry has proven to be an especially promising method for studying the mechanisms of electrochemical processes. The new 3D representation of the data can be effectively used in order to reveal the formation of electroactive species at the disk electrode. By using appropriate potential programs, the selectivity and sensitivity of RRDE systems can be significantly increased. The results of some selected experiments have been discussed and some drawbacks of the technique have been pointed out. Numerical simulations have been carried out in order to study the cross-talk effects, and a method has been suggested for their reduction.

1. Introduction

When studying the mechanisms of electrochemical processes, one of the most convenient and widely used methods of determining the reaction pathway is an electrochemical assay of the reaction products using a rotating ring–disk electrode (RRDE) [1-7]. The first RRDE was developed by Frumkin, Levich and their coworkers in 1959 [8].

As a typical example of the so-called generator-collector assemblies, an RRDE tip consists of two electron conducting parts: a generator, the centrally located disk, and the collector, the ring around it. The disk and the ring are separated by a gap that is usually made of the same insulating material as the outer cladding (Figure 1), and they can be connected to a bi-potentiostat [9] through separate leads. The development of the rotating disk electrode with a concentric ring provides a means of accurately defining and controlling the rate of diffusion of a soluble electroactive species and detecting in a quantitative manner the nature and amount of an electroactive species which is formed as an intermediate or product.

In fact the ring–disk electrode is a combination of an ordinary rotating disk electrode (RDE) with a ring electrode. (the term “ring electrode” usually refers to the case where the region $r_2 \le r \le r_3$ is active with respect to the surface process (r is the radius measured from the center of the cylindrical tip). This means that the regions $0 \le r < r_2$ and $r_3 < r \le r_0$ are inactive. The essential feature of this system is that there is an inactive region at the center of the disk.)

The lower surface of the actual RRDE tip is divided into active and inactive regions, as follows:

(*i*)	$0 \le r \le r_1$	→	active
(*ii*)	$r_1 < r < r_2$	→	inactive
(*iii*)	$r_2 \le r \le r_3$	→	active
(*iv*)	$r_3 < r \le r_0$	→	inactive.

According to the theoretical considerations, r_1 must be sufficiently large so that the central region (*i*) functions as a disk. $r_3 - r_2$ must be small so that region (*iii*) functions as a

*langgyg@chem.elte.hu

ring. On the other hand the overall radius of the tip (r_0) must satisfy the fluid-flow requirements i.e. r_0 is much greater than the thickness of the so-called momentum boundary layer [10].

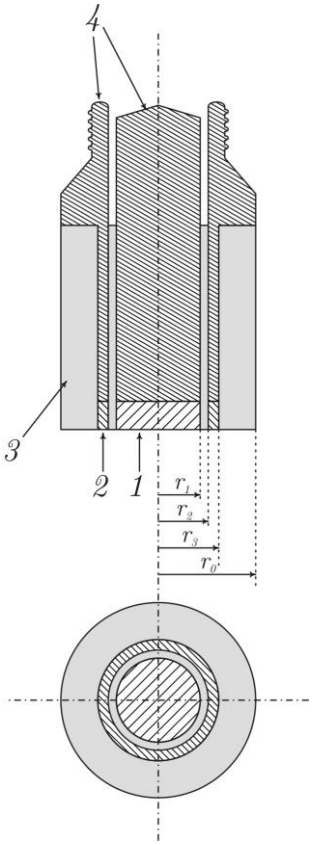

Figure 1. Rotating ring–disk electrode. *1:* disk electrode material, *2:* ring electrode material, *3:* insulator, *4:* metal support, r_1*:* disk radius, r_2*:* inner ring radius, r_3*:* outer ring radius, r_0*:* overall radius of the tip.

The fact that the potentials of the two electrodes can be controlled independently makes the RRDE a very powerful device of detecting and exploring the behavior of electroactive intermediates or products of electrode reactions, and when properly operated with the aid of a bi-potentiostat, it can effectively be used even for the detection of short-lived intermediates.

The popularity of the RRDE technique results from several considerations [11]: an adequate theory has been available for a long time, the RRDE has the advantage of well-controlled hydrodynamics and the rate of mass transport can be varied easily by varying the rotation rate, the electrodes can be easily cleaned and polished, the RRDE is placed in a recipient that can easily be deaerated and thermostated.

The RRDE takes advantage of the radially directed laminar flow created during its rotation. Any intermediates or products generated by some electrochemical reaction taking place at the disk electrode will be swept away by the flow towards the side of the electrode. Since the flow of the products passes nearby the ring, if some of these species are electrochemically active, they might be detected with a good chance at a ring potential appropriately chosen. Imagine that the disk electrode is set to pass a given (constant) current I_D, which generates a constant flux of species (intermediate), and the ring electrode is set at a potential such that all intermediate that reaches it is destroyed, i.e. the concentration of the intermediate at the ring is zero. Some amount of the intermediate will escape into the bulk of

the solution and so the ring current (I_R) will be only a fraction of the disk current. The fraction $N_0 = | I_R / I_D |$ is called the collection efficiency.

Despite many advantages, there are some drawbacks and practical inconveniences concerning the application of RRDEs. For example, the collection efficiency of other generator/collector devices (such as array electrodes) is higher, which gives microelectrode systems an advantage in detecting small amounts of generator electrode products. On the other hand, it is a considerable advantage of the RRDE that in experiments employing this technique the hydrodynamic constraints assure that the current-potential characteristics of the generator electrode remain unaffected by the presence of the collector; which is not the case when using other devices, microelectrode systems included.

So far, when the RRDE was used to detect intermediates of electrode reactions, mainly one of the following techniques were used [1-9,11-13]:

- A current-potential curve was recorded at the disk while the ring potential was held at a constant value where the intermediates or products are reduced or oxidized.
- The disk was held at a potential where intermediates or electroactive products were formed and the ring was maintained at a potential at which they have undergone electron transfer.
- The disk was held at a potential where the reaction of interest took place, and a current-potential curve was then recorded at the ring.
- The subject of observation was the transient shielding of the ring current for the electrolysis of a species upon stepping the disk potential to a value where this species was adsorbed.

The common feature of all the above techniques is that the potential of at least one of the two electrodes is held constant during the experiment.

However, independent and dynamic potential programs can also be applied (simultaneously) to the disk and the ring electrodes, e.g. while one electrode conducts linear sweep voltammetry the potential of the other can be also swept in a controlled manner. In this case one may expect that by applying appropriate potential programs, the selectivity and sensitivity of RRDE system can be increased [7].

2. Measurement setup and measuring techniques

To carry out dual dynamic voltammetry experiments a computer-controlled multi-channel electrochemical measuring system is necessary. In the experimental setup described in [7,14-16] the basis of the system is formed by National Instruments data acquisition cards, combined with commercially available potentiostats and other laboratory devices, such as electrode rotating units, quartz crystal microbalances, etc. Figure 2 shows the scheme of a typical experimental setup.

In the experiments reported in [7,14-16] “PINE AFE7R8” RRDE tips were used with a bi-potentiostatic setup of XPot devices manufactured by ZAHNER-Elektrik, Kronach, Germany; both the ring and the disk were made of polycrystalline gold. The gap size between the ring and the disk was 178 μm and the collection efficiency of the RRDE was 22%.

Special care was taken in order to overcome problems that might be caused by impurities in the system. The electrode surface was firmly polished with a “Struers DP-Suspension, P” polishing suspension that contains monocrystalline diamond of a granular size of ¼ μm. The electrode was then rinsed with pure ethanol and Milli-Q water, and in order to thoroughly remove all traces of contamination from the surface, it was cleaned ultrasonically for several minutes and washed extensively with ultrapure water. Every glass parts used in the experiments were immersed in Caro’s acid, rinsed in de-ionized water, and cleaned by steam. The software controlling the electrochemical workstation was programmed in the National Instruments LabVIEW environment. The software can not only be used to define any kind of potential-controlling waveforms (provided that these can be defined either as a closed-form

expression, or as a combination of simple periodic functions), but it also allows to represent and evaluate the measured data in several ways.

The experimental setup discussed above allows the application of the following experimental techniques:

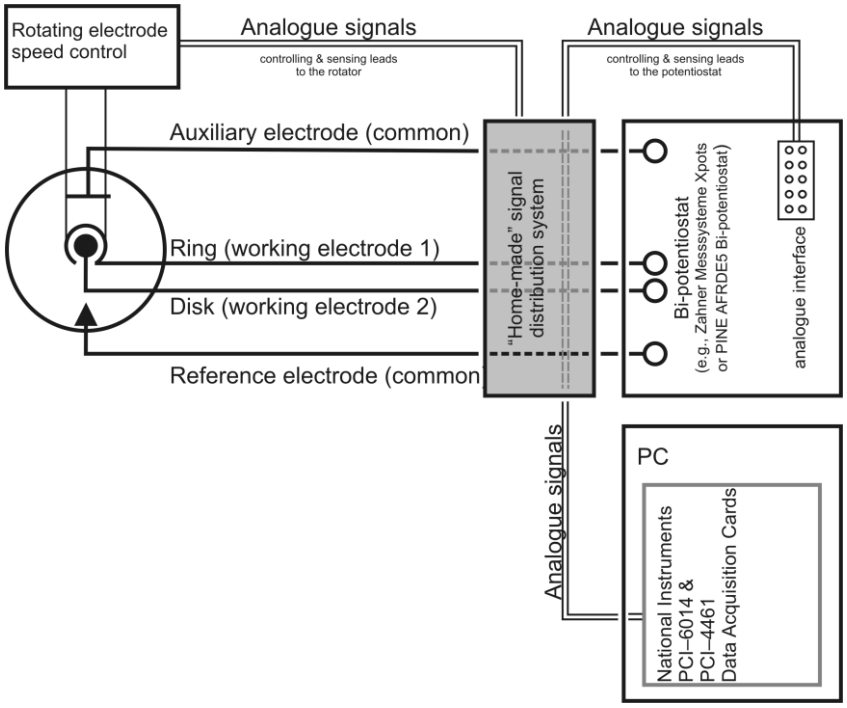

Figure 2. Scheme of the measuring system.

2.1 Phase shifted dual cyclic voltammetry

In the experiments reported in [7], the symmetrical triangular waveforms driving the potentials of the two electrodes were identical (the vertex potentials and the potential sweep rates for the two signals were the same), but the phases were different. An interesting result was that detectable amounts of reducible gold-containing species are leaving the oxidized gold surface during the reduction of the surface oxide layer in H_2SO_4 solutions.

2.2 Independent cyclic potential scans at the ring and disk electrodes

The potential programs applied to the disk and the ring electrodes can differ quite considerably; e.g., the "disk electrode" can be polarized at a sufficiently low and the "ring electrode" at a sufficiently high scan rate. In this case a 3D map can be constructed, which may reveal the electroactive intermediates or products that are formed in the electrode process(es) taking place on the disk [14-16]. This technique has been tested using the Au | 0.5 M H_2SO_4(aq.) system (under air-saturated and deaerated conditions) as an illustrative example [14-15], i.e. the oxygen reduction process has been chosen as model reaction.

2.3 Application of arbitrary waveforms, alternating potential and current transients

The study of ring–disk electrode transients can provide the means by which the flux of electrons, the disk current, and the flux of material at the disk surface can be measured independently. This means that at any time in the transient one can measure the proportion of the current that is actually producing electroactive intermediates in the solution. For instance, if an alternating current is passed through the disk electrode then an alternating current may be seen on the ring [1]. On the other hand, by applying a small a.c. signal to the ring

electrode, the impedance of it can be determined, e.g. as a function of the disk potential. In addition, by measuring the impedance of the ring electrode over a range of frequencies, an impedance spectrum can be constructed. Such impedance spectra may provide information not only about the electrochemistry of the electroactive intermediates or products, but also about ionic or neutral species which leave the disk electrode, and adsorb at the ring electrode in such a way that they change the value of a characteristic (e.g. the double-layer) capacitance.

3. The evaluation of RRDE experiments based on "dual potentiodynamic perturbation" techniques

The interpretation of rotating ring–disk experimental results often presents a challenge from a data analysis standpoint. RRDE experiments involve the examination of two potentials (that of the disk, E_{disk}, and that of the ring, E_{ring}) and two currents (I_{disk} and I_{ring}), thus the representation of the results calls for more dimensions than for experimental results involving a single working electrode only [3]. Of course in the case of "classical" RRDE techniques, where at least one of these variables is held constant (and furthermore, the attention of the experimenter is usually confined to stationary processes), the afore-mentioned multi-dimensionality is not an issue in itself. The case becomes more complicated if the experiment is based on the application of a transient technique, where time needs to be handled as a variable as well; and much greater difficulties can arise when *both* the generator and the collector electrodes are perturbed by time-varying controlling waveforms. In this case neither the disk, nor the ring electrode responses remain stationary, which makes the interpretation of the measured data a challenging task indeed.

In this section we demonstrate how a meaningful representation of such experimental results may become possible by referencing the measured ring electrode signals showing collection effects to a case when no such effects are present in the signal. Two different strategies of referencing will be presented in this section; however, they are both applied with the same aim. The goal in both cases is to "remove" signals from the collector electrode characteristics that are attributed solely to the electrochemical behaviour of the collector (ring) electrode itself, and thereby revealing the current signals which are on the other hand caused by actual collection or shading effects.

- The detection of disk electrode products formed in high amounts.

  One of the methods presented below has proven to be especially powerful for the detection of products and side-products that are formed in a relatively high amount in the disk electrode reaction, and give a ring current also of a high intensity. The basic idea of this method is that the big collection-related ring signals can be well detected even if the "ring current baseline" itself is of considerable intensity. The application of this method calls for the continuous scanning of a broad window of ring electrode potentials, while the disk is polarized at a slow rate. The method facilitates the detection of various disk electrode products as a function of both the disk and ring potentials and results in a "three dimensional map" of the species formed in the disk electrode reaction. In case of this method, the changes of the measured "ring CVs" are detected and compared to a reference curve which was recorded at an "inert" disk potential.

- The detection of disk electrode products formed in small amounts.

  In case the generator electrode yields only a small amount of detectable intermediates, the measured ring currents related to the collection of these species remain small as well. However, the RRDE methods based on the dual potentiodynamic perturbation of both working electrodes can still prove to be useful in this case. For the successful

detection of small collection-related currents, the current baseline of the ring electrode has to be kept relatively low and special care needs to be taken in order to avoid the misinterpretation of "pseudo-collection" effects which are often present, and are caused by an electrical crosstalk between the generator and collector electrodes. In this case, it is usually the comparison of ring currents measured at a rotating and a stagnant electrode that offers a possibility of meaningful representation of the results.

In this section both of the above mentioned strategies of representing the measured data will be demonstrated on the example of the gold | sulphuric acid system. For demonstration purposes, a simple gold disk-gold ring RRDE was used in contact with a 0.5 mol·dm^{-3} sulphuric acid solution. A saturated calomel electrode (SCE) served as a reference, and a gold plate with large surface area was used as a counter electrode. (For further experimental details, see [16].)

3.1 Creating a 3D map of electrode reaction products and side-products

The basic idea of this technique is that a linear potential sweep (of low rate) is applied to the disk electrode, while cyclic voltammograms (of a relatively high sweep rate) are measured at the ring. The results of such experiments can lead to the creation of a "3D map", which may reveal the electroactive intermediates or products that are formed in the electrode process(es) taking place on the disk. The applicability of the proposed technique is demonstrated here by considering the oxygen reduction process at the gold | 0.5 mol·dm^{-3} sulphuric acid electrode as an illustrative model reaction.

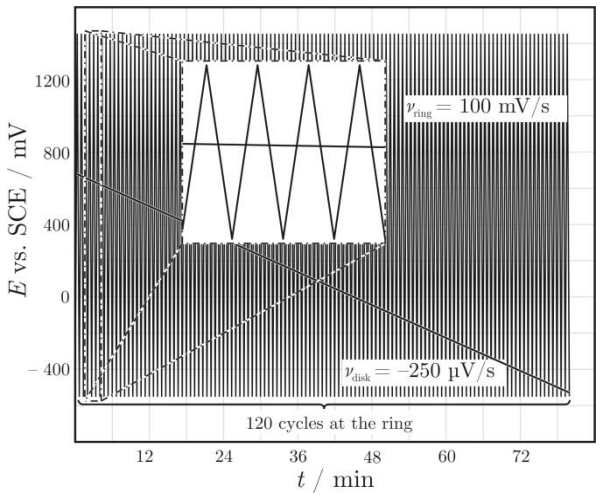

Figure 3. Controlling waveforms of the disk and ring electrodes: while the disk potential is slowly swept towards cathodic values, a multitude of cyclic voltammograms are obtained from the ring with a high sweep rate.

Figure 3 shows the controlling waveforms applied to the disk and ring electrodes of the RRDE in use (the cell itself was saturated with air during these measurements), while Figure 4 shows the measured disk polarization curves and the ring CVs.

The oxygen reduction reaction at gold surfaces has been extensively studied in the literature, and it has been established that in acidic media, the process usually involves the formation of H_2O_2. The peroxide intermediate is reduced to water only at more negative potentials. Whether the $2e^-$ or the $4e^-$ process is more favourable on a polycrystalline gold surface is known to be a function of the electrode potential and the pH; however, to identify the potential region at which the two-electron pathway is dominant is not always straightforward. The application of the dual potentiodynamic perturbation technique makes it

possible to estimate the disk potential at which the maximum amount of peroxide is formed, and thus can yield useful information regarding this matter.

The experiment was carried out as follows: The disk electrode was slowly polarized from 600 to −600 mV vs. SCE (at a sweep rate of 0.25 mV/s), while the cyclic voltammograms of the ring were recorded at a sweep rate of 100 mV/s between the potential limits of 1450 and −550mV (Figure 3). The electrode was rotated at 1000 rpm during the experiment.

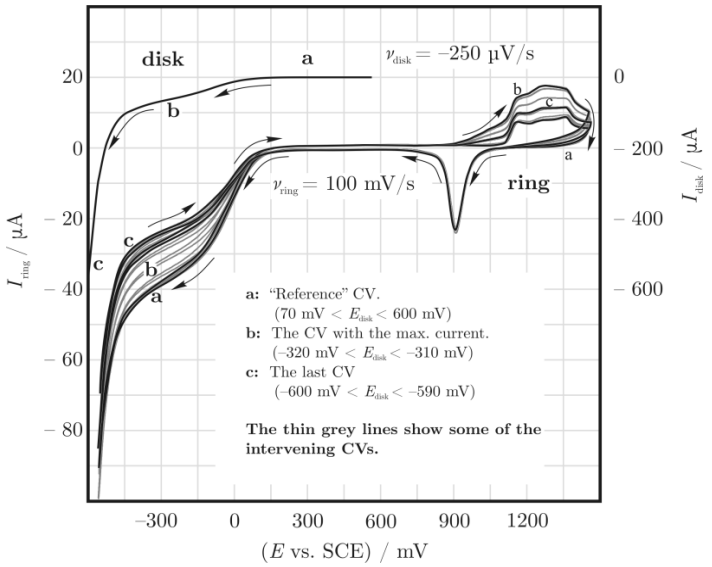

Figure 4. The shape of the CVs measured on the ring change when oxygen reduction occurs on the disk electrode in an air saturated 0.5 mol·dm^{-3} H_2SO_4 solution. The polarization curve obtained from the disk and a few ring CVs are shown together, rotation rate: 1000 rpm.

As it can be seen in Figure 4, at the beginning of the disk scan, while the disk potential is more positive than the negative potential limit of the double-layer region, the cyclic voltammograms measured at the ring are characteristic for a clean polycrystalline Au electrode, and show no "collection-related" effects. However, as the disk potential becomes more and more negative, significant changes of the ring CVs can be observed. One of these observable features is that the absolute values of the cathodic ring currents measured at negative ring potentials begin to decrease as the reduction of oxygen begins on the disk. This effect is termed *shielding*, and is a result of the fact that with decreasing disk potentials, the oxygen content of the solution reaching the ring electrode also decreases. The "intensity of shielding" thus indicates the lack of oxygen in the solution that is caused by the disk electrode process.

Apart from the shielding effect, signs of actual collection can also be seen on the ring CVs of Figure 4. This effect can be seen at positive ring potentials in the form of an anodic current. The anodic current is attributed to the fact that the H_2O_2 formed at the disk can get oxidized on the ring electrode, if its potential is positive enough. The signal begins to appear as the disk potential gets to approximately 70 mV, and increases continuously until the disk potential reaches the value of approximately –310 mV. However, a notable feature of this effect is that as E_{disk} gets even more negative, the measured ring signals begin to decrease again.

It can be seen from the above, that in case of these measurements, it is the *deviation* of the ring electrode CVs (measured from their "normal shape") which carries information on the collection and/or shielding effects. More formally, it is the current difference

$$\Delta I_{\text{ring}}\left(E_{\text{disk}}, E_{\text{ring}}\right) = I_{\text{ring}}\left(E_{\text{disk}}, E_{\text{ring}}\right) - I_{\text{ring}}\left(E_{\text{disk}}^{\text{ref}}, E_{\text{ring}}\right), \quad (1)$$

a function of both the disk and the ring potentials, which contains this information. In Eq. 1, $E_{\text{disk}}^{\text{ref}}$ can be any arbitrarily chosen disk potential, at which the disk electrode can be considered as "inert" or "inactive", and thus the measured ring CVs have their "normal" shape (i.e. uninfluenced by the disk electrode).

In order to estimate the ΔI_{ring} values as a function of the disk and ring potentials, our attention will hereafter be confined to the anodic ring sweeps (as it can be seen in Figure 4, the deviations are much more pronounced in this case). As the referencing of Eq. 1 is not directly possible (E_{disk}, E_{ring} and I_{ring}, the variables that need to be treated here are recorded in such a way that the measured data are equidistant with respect to time and not with respect to the disk and ring potentials), the application of two dimensional interpolation techniques becomes necessary. This interpolation can be carried out based on a general formula

$$I_{\text{ring}}\left(E_{\text{disk}}, E_{\text{ring}}\right) = \sum_k I_k L\left(E_{\text{disk}} - D_k, E_{\text{ring}} - R_k\right), \quad (2)$$

where I_k, D_k and R_k denote the measured ring current, disk potential and ring potential values of the k^{th} row of the measurement records, respectively. In practice, the summation is only carried out for those k entries, for which both $\left|E_{\text{disk}} - D_k\right|$ and $\left|E_{\text{ring}} - R_k\right|$ are less than a specified small value denoted by a.

The bivariate function $L(x, y)$ introduced in Eq. 2 is called the interpolation kernel, and its definition depends on the resampling method we use. In general, $L(x, y)$ should be a radial basis function, thus

$$L(x, y) = L(x) \cdot L(y). \quad (3)$$

In practice, many types of kernel functions can be used (and were tested); however, based on our experience, the best results can be achieved by the application of the so-called Lánczos-kernel defined as

$$L(x) = \begin{cases} \operatorname{sinc}(x) \cdot \operatorname{sinc}\left(\frac{x}{a}\right) & \text{if } |x| < a \\ 0 & \text{otherwise} \end{cases} \quad (4)$$

where $\operatorname{sinc}(x) = \dfrac{\sin(\pi x)}{\pi x}$ is the normalized sinc function.

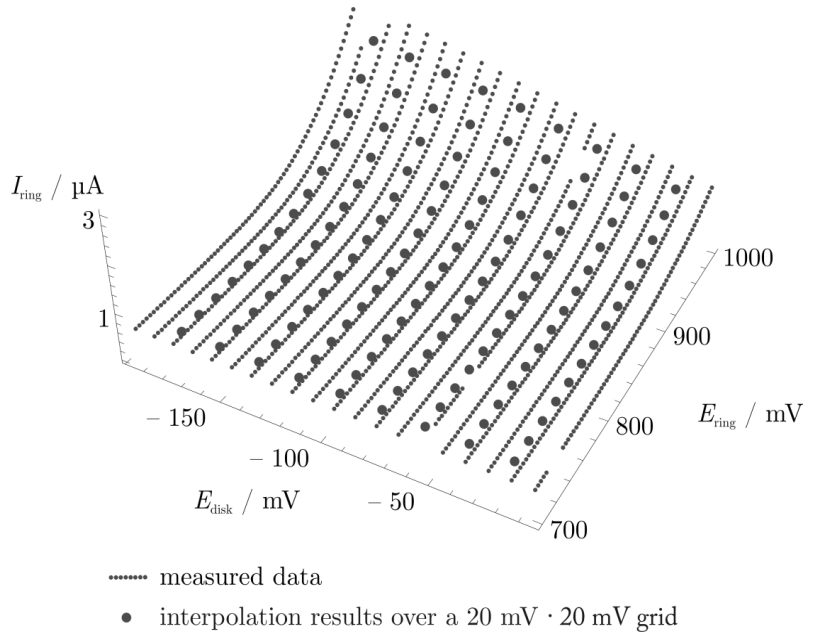

Figure 5. Interpolation results (shown here only over a small segment of the measured data). The measurement records, equidistant with respect to time, are resampled to yield the interpolation results that are equidistant with respect to the disk and ring potential.

The interpolation using the Lánczos kernel was applied to the measured data presented in Figure 4 (like it was mentioned before, only the data recorded during the anodic ring sweeps were used), and the I_{ring} values were calculated over a 20 mV · 20 mV square-grid of $-600\,\text{mV} \le E_{\text{disk}} \le 600\,\text{mV}$ and $-600\,\text{mV} \le E_{\text{ring}} \le 1450\,\text{mV}$ (see Figure 5).

Following the interpolation, the ring currents measured at $E_{\text{disk}}^{\text{ref}} = 600\,\text{mV}$ were taken as a reference curve, and the subtraction based on Eq. 1 was carried out on the resampled dataset in order to acquire the ΔI_{ring} surface presented in Figure 6.

Such a representation (Figure 6) can be used in order to detect electroactive species which are generated at the disk electrode with an increased efficiency compared to the traditional "constant ring potential" techniques, and it can be interpreted as a three-dimensional map of the intermediates or products of the electrode process under study. In case of the oxygen reduction process, the method can be used e.g. to estimate at which disk potential the highest amount of hydrogen peroxide is leaving the disk electrode, and at which ring potentials it can be effectively detected. As it can be seen in Figure 6, "Peak A" represents the reduction of O_2 and (ΔI, now the difference between two negative currents, turns out to be positive here), and "Peak B" the oxidation of H_2O_2 at sufficiently positive ring potentials.

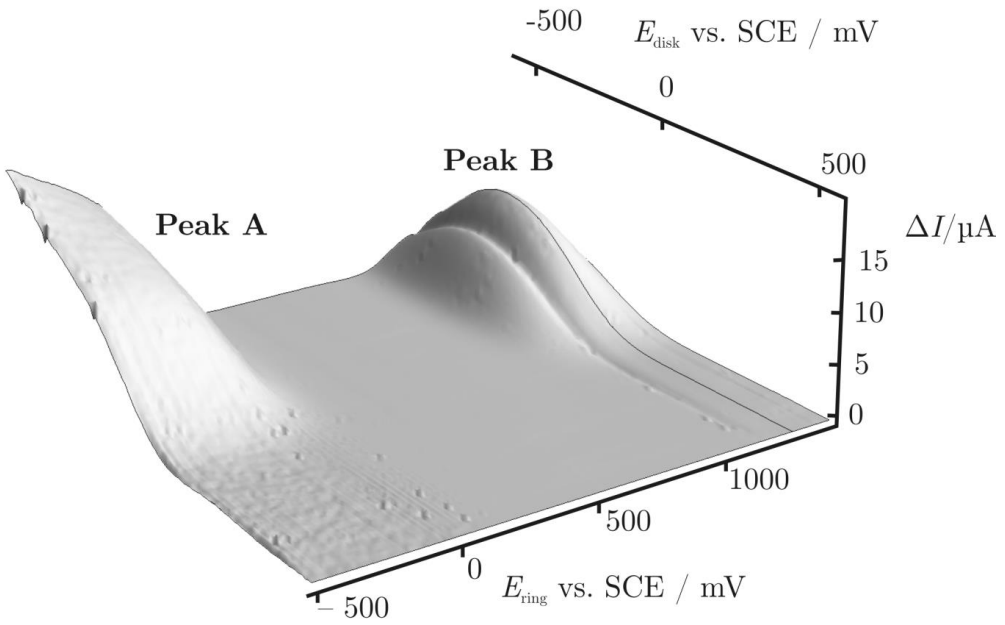

Figure 6. Differences of the ring current (ΔI) measured from the "normal anodic scan" measured at E_{disk} = 600 mV. ΔI is a function of E_{disk} and E_{ring}. Peak A corresponds to the "lack of reducible O_2" caused by the oxygen reduction on the disk, while peak B corresponds to the oxidation of the H_2O_2 coming from the disk.

For instance, it has been concluded in studies found in the literature [17] that in case of a gold disk with a gold ring "nearly all of the H_2O_2 formed diffuses away from the disk into the solution and produces little current at the ring". However, our method presented here can clearly show that the H_2O_2 formed at the disk can be effectively detected at the ring when sufficiently positive potentials are applied (see the mentioned Peak B in Figure 6).

3.2 The application of dual cyclic voltammetry in small-signal collection experiments

In the above example, the bi-potentiodynamic perturbation of the RRDE was applied in order to detect side-products of the disk electrode reaction that are formed in a relatively big amount. The shielding effect caused by the oxygen consumption and the collection effect caused by the H_2O_2 formation at the disk electrode were both of considerable intensity: the differences in the measured ring current were significant even when compared to the "normal" ring CVs.

This is however not the case when the disk electrode reaction yields only a small amount of detectable intermediates. The collection of these species leads to the appearance of a small collector current only, which is in the range of the small ring current baseline distortions caused by the electrical crosstalk between the disk and the ring.

This crosstalk is a result of the uncompensated *IR* drop effect [18] that has a more complex nature in two working electrode systems compared to a standard three-electrode cell. In order to make proper distinctions between ring signals arising from an actual "collection" (which is the subject of interest), and signals resulting from the crosstalk of mere electrical nature, special care needs to be taken.

The Au | 0.5 mol·dm^{-3} H_2SO_4 system will again serve as an illustrative example in order to demonstrate the effect electrical crosstalk can exert on RRDE measurement results. It was described in 1974 by Cadle and Bruckenstein [19] that during the reduction of the oxide layer covering the surface of the disk electrode of a gold disk/gold ring RRDE, at least one soluble, electroreducible species is escaping from the disk and can be collected at the ring. It was shown by the same authors (by the application of an RRDE that consisted of a gold disk and a platinum ring) that the mentioned intermediate is oxidized gold, and this finding was also

confirmed elsewhere by the application of TXRF and ICP-MS analysis which showed the presence of dissolved gold in the solution. [7]

The approach that Cadle and Bruckenstein used for the detection of the soluble gold species was based on the measurement of cyclic voltammograms at the disk electrode, while holding the ring at sufficiently negative potentials. The technique presented in [19] will be discussed below, and it will be demonstrated how the sensitivity and the applicability of the RRDE detection can be extended by the application of dual dynamic perturbations.

The following experiments were carried out by using the same setup as before; however in this case the solution was carefully deaerated by Ar gas and an inert gas blanket was maintained over the electrolyte solution throughout the experiments.

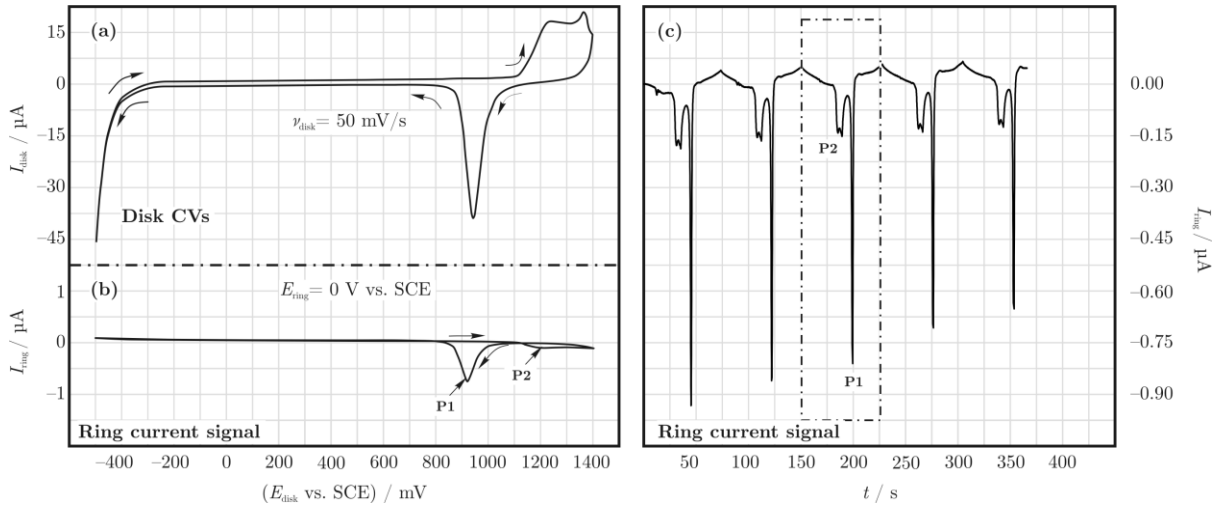

Figure 7. (a) Cyclic voltammograms measured on the disk electrode between vertices of 1400 and –500 mV at a sweep-rate of 50 mV/s. (c) The ring current is recorded in parallel with measuring the CVs of the disk. A segment of the measured ring current is shown as a function of the disk potential in (b). Rotation rate: 500 min^{-1}.

Figure 7 (a) shows several cyclic voltammograms obtained at a sweep rate of 50 mV/s from the disk electrode (vertices: −500 and 1400 mV), and Figure 7 (b) shows the ring current that was measured while recording a selected disk CV (the ring electrode was held at a potential of 0 V vs. SCE during the measurements and the electrode was rotated at a rate of 500 min^{-1}).

As shown in Figure 7, two small cathodic peaks can be observed in the measured ring current curves. These peaks (denoted with P1 and P2 in Figure 7(b) and 7(c)) appear in parallel with the reduction of the surface oxide layer and the formation of the surface oxide, respectively. However, as it is clearly visible in Figure 7(c), the intensity of the detected peaks significantly decreases with the number of potential cycles applied to the disk. As in the meantime the disk CVs themselves do not change, this indicates that the electrocatalytic activity of the ring electrode decreases remarkably with time (most probably due to contaminations from the solution). This is certainly an issue which makes the reproducibility (and also the quantitative interpretation) of the measurements questionable.

In addition we should also note that the aforementioned sensitivity loss is not the only issue here. It is also clearly visible in Figure 7(c) that the shape of the "ring current baseline" is not very well-defined. Several difficulties may arise from this fact, especially if we would like to determine the amount of the collected intermediates by the means of numerical integration.

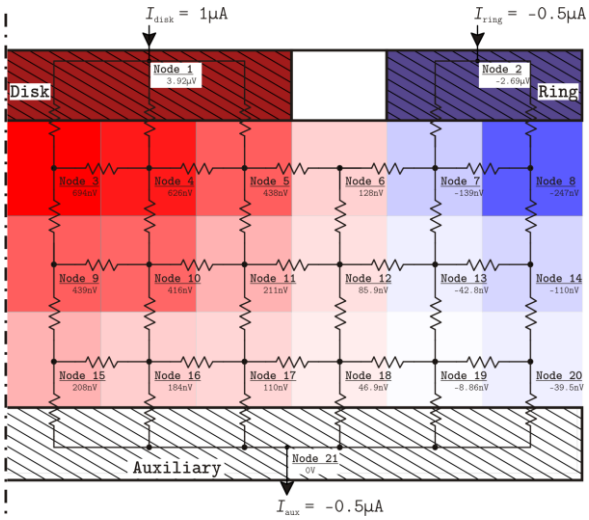

Figure 8. Illustration of the results that nodal analysis on a given simulation grid can yield. The potential values (positive for warm colours and negative for cold colours) are different throughout the simulation mesh: the *IR*-drop affecting the 2 working electrodes thus depends on the position of the Luggin capillary. (S. Vesztergom, unpublished results.)

As it was shown by simulations carried out on an RRDE equivalent circuit [16], the observed instability of the baseline can be related to an electrical crosstalk that is introduced to the system by a shared current route of the two working electrodes. This issue was discussed extensively by Dörfel *et al* [20]. They pointed out (based on theoretical treatment and also on experiments) that the observed *IR*-drop effects in an RRDE system can be treated as a sum of "normal ohmic drop" and "ring–disk coupling" effects, and that the extent of these impacts is heavily affected by the position of the *Luggin*-capillary with respect to the RRDE geometry. The authors were discussing galvanostatic experiments and suggested that the resulting potential *vs.* time curves should be corrected by a simple parallel shift; on the other hand, they concluded that the subsequent correction of a potentiostatic current *vs.* potential curve "is far more difficult or even impossible". To this we add that the (analytical) description of *IR*-drop effects in an RRDE system can indeed be very challenging; however, if we give up our demands for an analytical solution, a theoretical (numerical) treatment may become possible. In order to achieve this, we should start from one of the classical digital simulation approaches. For example in [21] a finite-element method was successfully used in order to describe convection and diffusion over a given simulation grid. The method presented there can be extended by using the simulation grid itself as an "equivalent circuit" over which a nodal analysis can be carried out (by using the currents I_{disk} and I_{ring}, as well as the charge transfer and solution resistances as parameters) in order to estimate the electric potential field at each points of the simulation mesh.

This approach is demonstrated by Figure 8, showing the results that the nodal analysis of a given simulation grid can yield. In this calculation, currents of 1 µA and –0.5 µA were assumed to flow through the disk and ring electrodes, respectively, and the resistance values were all set to 1 Ω (except for the "charge transfer" resistances crossing the disk or the ring boundary, which were given a value of 10 Ω). The results presented here serve demonstration purposes only: a real simulation is carried out on a much denser grid, and the current as well as the resistance values are time-dependent and are continuously calculated as the simulation is running. Still it can be seen in Figure 8 that the ohmic potential drop affecting the disk and the ring electrodes can indeed depend heavily on the position of the Luggin capillary.

From the description above it becomes visible that *IR*-drop effects in case of an RRDE are indeed of a complex nature, and even issues like positioning the reference electrode may become a compelling factor to the success of the experiments. This can be easily proven: for example, if we carry out the same measurements presented in Figure 7 but we place the

reference electrode to a not so well-chosen position, the presence of crosstalk immediately becomes more obvious (results are shown in Figure 9; here the Luggin capillary was placed 'too close' to the disk electrode).

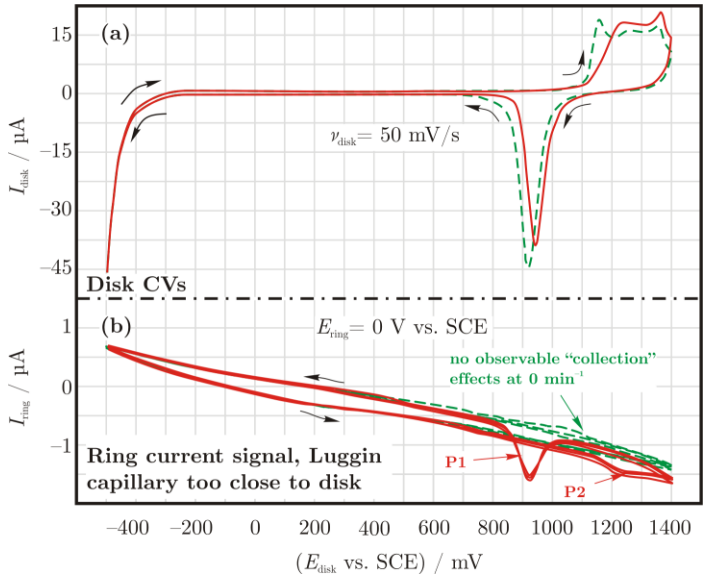

Figure 9. The measurements of Figure 7 repeated with a not suitably placed Luggin capillary: the effect of electrical crosstalk is much more visible here. Note that the crosstalk effect remains present also if the electrode is not rotated (green curves), but in this case no collection of the intermediates appears. (Collection-related signals are present only in the red curves recorded at a rotation rate of 500 min^{-1}.)

To conclude, we can say that during the quantitative evaluation of "small-signal" collection experiments, difficulties can arise because of two main reasons: *i.)* that the detected current peaks decrease with time (most probably due to contaminations accumulating at the electrode surface, as it was mentioned above with reference to Figure 7) and *ii.)* that due to the significant electrical crosstalk, ring current baseline is also of considerable intensity, which may cause a significant error in the numerical integration (numerical integration is often applied to calculate the "charge" carried by the intermediates).

The above mentioned difficulties can be successfully overcome, again, by the simultaneous application of dual dynamic perturbing waveforms to both the disk and ring electrodes. An example of this technique is described below.

The measurements presented in Figure 10 were carried out by recording cyclic voltammograms not only of the disk, but also of the ring electrode at the same time. Similarly to the measurements presented before, the disk was polarized at a rate of 50 mV/s between vertices of −500 and 1400 mV vs. SCE. Simultaneously, the ring CVs were taken within the boundaries of the double-layer region, between 200 and 675 mV, at a rate of 12.5 mV/s. The triangular waveforms controlling the potentials of the disk and ring electrodes were therefore synchronous (meaning that they both had a frequency of $f = {}^{1}/_{76}$ Hz), and a phase shift of 180° was introduced in-between them (see the inset of Figure 10).

It can be seen in Figure 10 that both the disk and the ring CVs have a different shape when the electrode is stagnant (non-rotating, marked with a green dashed line) and when it is rotated at a frequency of 500 min^{-1} (solid red line). Similarly to Figure 9, the effect of crosstalk is still present, and this becomes readily visible if we compare the two ring CVs to the dotted curve shown in Figure 10(b). (The dotted curve is a "crosstalk-free" cyclic voltammogram of the ring that can be recorded while the disk is at open circuit). It can also be seen that the crosstalk influences the ring CVs in practically the same manner, regardless to the rotation rate.

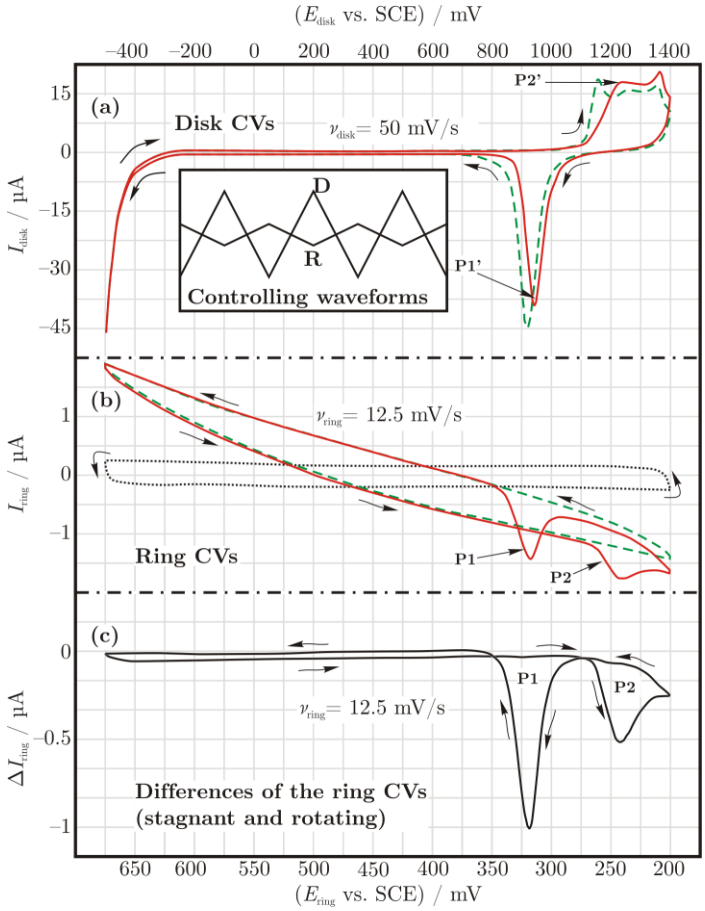

Figure 10. Multiple consecutive (however overlaying) cyclic voltammograms obtained simultaneously from the disk (a) and the ring (b) electrodes. Solid (red) and dashed (green) lines mark the measured CVs when the electrode is rotating (at 500 min^{-1}) and when it is stagnant, respectively. The dotted curve in (b) shows a cyclic voltammogram of the ring when the disk electrode potential was not controlled: no electrical cross-talk can be seen in this curve. The plot in (c) shows the difference between the solid and dashed curves in (b).

It can also be seen in Figure 10(b) that if the RRDE tip is rotated (red curve), the two peaks we have seen before (marked with P1 and P2) can be observed in the ring CV. Since the triangular perturbations of the two electrodes are synchronous (they are of the same frequency) and they are shifted with 180° with respect to each other, the points of each curves in Figure 10 with a matching horizontal coordinate coincide with each other in time. It should be noted that the applied method offers a possibility of distinguishing between currents due to the electrical cross-talk effects and faradaic currents corresponding to the collection of species. By subtracting the ring currents measured at a stagnant electrode from those measured when the electrode is rotating (i.e., by calculating the difference of the red and the green curves), the plot in Figure 10(c) can be created.

In this representation the intensity of the peaks P1 and P2 is much higher, compared to the conventional RRDE results presented in Figure 9, and the resolution is also significantly improved. It has to be emphasized, that a very important advantage of this technique is that by the continuous potential cycling, the ring electrode surface is kept clean and unlike the "constant ring potential" experiments, no sensitivity loss can be experienced. (The curve of Figure 10 (c) represents multiple overlaying ring CVs while in Figure 9 (c), only a segment of the (continuously changing) ring currents was shown.) Based on the application of this method we can confirm the results found in the literature, that the reducible species responsible for the peaks appearing in the ring current is mainly produced during the

reduction of the 2D surface oxide layer (see peak P1’ on the disk CV of Figure 10(a)); however we can also point out that the formation of the surface oxide yields reducible side-products as well (see peak P2’ in Figure 10(a)).

4. Conclusion

In the present study the dual dynamic voltammetry technique for rotating ring–disk electrodes has been discussed. It has been shown that the method of dual cyclic voltammetry (i.e. applying dynamic potential programs to the disk and the ring electrodes of an RRDE simultaneously) is a promising method for studying the mechanisms of electrochemical processes. The simultaneous perturbation of the disk and ring electrode potentials of an RRDE with time-varying controlling waveforms is an efficient way to carry out high-sensitivity collection experiments. The 3D representation of the data can be effectively used to reveal the formation of electroactive species at the disk. Unfortunately, the transients caused by the “dual dynamic” perturbation of the electrodes often results in electrical cross-talk effects between the two working electrodes. With the help of numerical simulations, it could be shown that this cross-talk is caused by the common resistance shared by the current paths of the disk and the ring electrodes. It has also been shown that the comparison of ring currents measured at a rotating and a stagnant electrode offers the possibility for the elimination of the undesirable effects from the experimental results.

Acknowledgement

Financial support from the Hungarian Scientific Research Fund (OTKA-PD75445&K109036, OMFB-01078/2007) and MKB Bank Zrt. (Budapest) is gratefully acknowledged. The authors thank National Instruments Hungary Ltd. for the donation of data acquisition cards.

References

[1] W.J. Albery and M.L. Hitchman, *Ring-disc electrodes*, Clarendon Press, Oxford, 1971.

[2] V.Y. Filinovsky and Y.V. Pleskov, Rotating disk and ring–disk electrodes. In: E. Yeager, J.O'M. Bockris, B.E. Conway and S. Sarangapani (eds), *Comprehensive treatise of electrochemistry* **9**, 293–352, Plenum, New York, 1984.

[3] A.J. Bard and L.R. Faulkner, *Electrochemical methods. Fundamentals and applications*, Wiley, New York, 2001.

[4] A.J. Arvia and S.L. Marchiano, Transport phenomena in electrochemical kinetics. In: J.O'M. Bockris and B.E. Conway (eds), *Comprehensive treatise of electrochemistry* **6**, 159–241, Butterworths, London, 1971.

[5] R.I. Holliday and W.R. Richmond, An electrochemical study of the oxidation of chalcopyrite in acidic solution, *Journal of Electroanalytical Chemistry* **288** (1990) 83–98.

[6] W. Zurilla and E. Yeager, Oxygen electrode kinetics on gold, *Technical report №3, AD 694951*, Office of Naval Research, 1969.

[7] S. Vesztergom, M. Ujvári and G.G. Láng, RRDE experiments with potential scans at the ring and disk electrodes, *Electrochemistry Communications* **13** (2011) 378–381.

[8] A.N. Frumkin, L.N. Nekrasov, V.G. Levich and Y.B. Ivanov, Die Anwendung der rotierenden Scheibenelektrode mit einem Ringe zur Untersuchung von Zwischenprodukten elektrochemischer Reaktionen, *Journal of Electroanalytical Chemistry* **1** (1959) 84–90.

[9] D.T. Napp, D.C. Johnson and S. Bruckenstein, Simultaneous and independent potentiostatic control of two indicator electrodes, *Analytical Chemistry* **39** (1967) 481–485.

[10] M.C. Wendl, *Theoretical foundations of conduction and convection heat transfer*, The Wendl Foundation, Saint Louis, 2012.

[11] S. Han, J. Zhai, L. Shi, X. Liu, W. Niu, H. Li and G. Xu, Rotating minidisk-disk electrodes, *Electrochemistry Communications* **9** (2007) 1434–1438.

[12] S. Bruckenstein and B. Miller, Unraveling reactions with rotating electrodes, *Accounts of Chemical Research* **10** (1977) 54–61.

[13] U.A. Paulus, T.J. Schmidt, H.A. Gasteiger and R.J. Behm, Oxygen reduction on a high-surface area Pt/Vulcan carbon catalyst: a thin-film rotating ring–disk electrode study, *Journal of Electroanalytical Chemistry* **495** (2001) 134–145.

[14] S. Vesztergom, M. Ujvári and G.G. Láng, RRDE experiments with independent potential scans at the ring and disk electrodes — 3D map of intermediates and products of electrode processes, *Electrochemistry Communications* **19** (2012) 1–4.

[15] S. Vesztergom and G.G. Láng, The construction of a novel electrochemical measuring system for enhanced rotating ring–disk electrode experiments, *Journal of Instrumentation Science and Technology* **41** (2013) 82–95.

[16] S. Vesztergom, M. Ujvári and G.G. Láng, Dual cyclic voltammetry with rotating ring–disk electrodes, *Electrochimica Acta* (2013). *In press*, http://dx.doi.org/10.1016/j.electacta.2013.01.142

[17] J.P. Hoare, Oxygen. In: A.J. Bard (ed), *Encyclopedia of electrochemistry of the elements* **2**, 321, Marcel Dekker, New York, 1974.

[18] M. Shabrang and S. Bruckenstein, Equivalent circuit for the uncompensated resistances occurring at ring–disk electrodes, *Journal of the Electrochemical Society* **121** (1974) 1439–1444.

[19] S.H. Cadle and S. Bruckenstein, Ring–disk electrode study of the anodic behavior of gold in 0.2M sulfuric acid, *Analytical Chemistry* **46** (1974) 16–20.

[20] Ch. Dörfel, D. Rahner and W. Forker, Studies of coupling effects and ohmic potential drops at ring-disc electrodes, *Journal of Electroanalytical Chemistry* **107** (1980) 257–270.

[21] K.B. Prater and A.J. Bard, Rotating ring–disk electrodes I. Fundamentals of the digital simulation approach. Disk and ring transients and collection efficiencies, *Journal of the Electrochemical Society* **117** (1970) 207–213.